PCCP

Matrix isolation FTIR and molecular orbital study of *E* and *Z* acetaldoxime monomers†

Agnieszka Andrzejewska,[ac] Leszek Lapinski,[bc] Igor Reva*[c] and Rui Fausto*[c]

[a] *Department of Chemistry, University of Warsaw, Pasteura 1, 02-093, Warsaw, Poland*
[b] *Institute of Physics, Polish Academy of Sciences, Al. Lotnikow 32/46, 02-668, Warsaw, Poland*
[c] *Departamento de Química, Universidade de Coimbra, 3004-535, Coimbra, Portugal*

Received 2nd April 2002, Accepted 7th May 2002
First published as an Advance Article on the web 7th June 2002

The molecular structures and vibrational spectra of the monomers of the *Z* and *E* acetaldoxime isomers were investigated by *ab initio* MP2/6-311++G** and DFT (B3LYP)/6-311++G** calculations. Experimentally, acetaldoxime was studied using FTIR spectroscopy combined with the technique of isolation in low temperature argon matrixes. Significant dependence of the ratio of *E* and *Z* isomers in the matrix on the method of sample preparation was observed. Matrixes with high predominance of the *Z* form were deposited, as well as such with dominating *E* form or with both forms in nearly the same amount. That allowed separation of the infrared spectra of both isomers. An assignment of the vibrational spectra of the two isomeric forms was based on comparison with the spectra theoretically calculated at the DFT and MP2 levels. The vibrational data were correlated with some important structural parameters, in particular the different methyl torsional barriers present in the two isomers.

Introduction

Aldoximes of general formula RHC=NOH (R = alkyl or aryl group) are important chemical and biological systems. Analogs of perillartine are reported to be responsible for both the sweet and bitter taste in humans.[1,2] Aldoximes are considered as prototype molecules for the general imine system R_1R_2C=NX and are found to be important substrates in stereoselective carbon–carbon bond forming reactions.[3] The simplest member of this family, formaldoxime (H_2C=NOH), is the only aldoxime with two identical substituents at the carbon atom and it does not show *E*–*Z* isomerism. One of the simplest aldoximes that can adopt *E* and *Z* forms is acetaldoxime (CH_3CH=NOH).

The relative energies of the *E* and *Z* isomers of acetaldoxime were previously calculated at the RHF/6-31G*,[4,5] RHF/DZ,[6] DFT(B3LYP)/6-31G* and MP2/6-31G* levels.[7] All these calculations predicted a small energy difference between the two forms. At the RHF/DZ and DFT(B3LYP)/6-31G* levels, the calculated energy of the *E* form was lower than that of the *Z* isomer by 2.5 and 1.7 kJ mol^{-1}, respectively, while the RHF/6-31G* and MP2/6-31G* calculations predicted the *Z* form as being slightly more stable (by 0.9 and 0.2 kJ mol^{-1}, respectively). Both *E* and *Z* isomers have been observed experimentally, by means of gas phase ^{1}H NMR spectroscopy,[8] for the compound in the vapour phase over the neat liquid. By integration of the signals due to OH protons, the relative population of the *E* isomer has been established as 40%. This value is close to the 37% reported for neat liquid.[9] Rogowski and Schwendeman[10] studied the microwave spectrum of gaseous acetaldoxime prepared by trap-to-trap distillation of the compound in vacuum. They observed both *E* and *Z* forms and, based on the tunnelling splittings of the spectral lines, estimated the heights of the barriers for methyl group rotation in both isomers. The barrier in the *Z* form was found to be very low (1.57 kJ mol^{-1}), while the corresponding value for the *E* isomer was significantly higher (7.68 kJ mol^{-1}). Dipole moments were also determined, with the *E* form being found to be slightly more polar [$\mu(E) = 0.938$ D; $\mu(Z) = 0.850$ D]. No experimental geometries of isolated acetaldoxime molecules in the *E* and *Z* forms were obtained in that study. The microwave study of deuterated *E*-acetaldoxime[11] confirmed the results of the investigations previously carried out for the normal species.[10]

^{1}H NMR data[12] indicate that at room temperature the *E*/*Z* population ratio in the neat liquid phase and in concentrated solutions is about 0.6. This population ratio was considered to be a measure of the average stability of different polymeric structures made by the two isomers in these phases, and not a measure of the relative stability of the monomeric forms.

The peculiar property of acetaldoxime is that at room temperature it can be either liquid or solid, depending on the history of the sample. Two crystalline varieties of the compound with different melting points (46.5 and 12 °C) were reported as early as 1892 by Dunstan and Dymond.[13] A high *Z*/*E* ratio up to 20 : 1 has been found in crystalline samples of acetaldoxime refrigerated for a long time.[14] *Z*-Acetaldoxime can be also prepared by slow crystallization of freshly distilled mixtures of isomers.[15] The kinetics of the conversion of the *Z* isomer, prepared in that way, to the "equilibrium" with 40% of the *E* form has been monitored in neat liquid by means of NMR spectroscopy.[15]

A solid sample of acetaldoxime, in which the molecules adopted exclusively the *Z* form, has been investigated by Okuda *et al.* using ^{14}N NQR spectroscopy.[16] At temperatures below 255 K no spectroscopic features ascribable to the presence of the *E* isomer were observed in the studied crystal.

Experimental infrared studies of acetaldoxime, reported so far, did not manage to differentiate between the *E* and *Z*

† Electronic supplementary information (ESI) available: Internal coordinates for the *Z* and *E* isomers, calculated barriers for the rotation of methyl groups and the relative energies of the relevant stationary points for acetaldoxime. See http://www.rsc.org/suppdata/cp/b2/b203240f/

absorptions, neither in condensed phases[17] nor in the gaseous state.[9]

In the present work we studied acetaldoxime in its *E* and *Z* forms by means of matrix isolation combined with FTIR spectroscopy. This technique, supported by theoretical calculations, allowed unequivocal identification and spectroscopic characterization of both isomeric forms of the compound.

Experimental

The sample of acetaldoxime, used in the present study, was a commercial product (Aldrich, 99%). Before cooling the cryostat, the ampoule with the compound was pumped several times for a few seconds at room temperature. The vapour pressure of acetaldoxime at 20 °C is 9.8 mm Hg. Thus, pumping at room temperature resulted in partial evacuation of the compound, but also in removal of the dissolved air and other volatile impurities. This approach allowed additional purification of the compound immediately before an experiment.

A glass vacuum system and standard manometric procedures were applied to deposit matrix gas (Argon, Air Liquid, 99.9999%), which was used without further purification. The argon deposition rate during sample preparation was *ca.* 5 mmol h^{-1}.

Spectra were recorded on a Mattson FTIR Spectrometer (Infinity 60AR series) in the range 4000–400 cm^{-1} with resolution 0.5 cm^{-1}. A DTGS Mid-IR detector and a KBr beamsplitter were used. All experiments were carried out using the APD Cryogenics closed-cycle helium refrigeration system with a DE-202A expander. Necessary modifications of the sample compartment of the spectrometer were made in order to accommodate the cryostat head and allow purging of the instrument by a stream of dry air to remove water vapours. A CsI window was used as the optical substrate for the matrixes.

At room temperature, acetaldoxime is a volatile compound and this allowed us to deposit some of the matrix samples using standard manometric techniques, when acetaldoxime was premixed with argon in a glass line. An alternative approach for preparation of matrix samples was the simultaneous deposition of argon, from the glass-line, and acetaldoxime, from the double-thermostatted Knudsen cell, described elsewhere.[18] The cell has two thermostattable parts: the valve nozzle and the sample compartment. The valve nozzle was kept at room temperature in all the experiments. Thermostatting of the compound at −39 °C, −19 °C and 0 °C was achieved by immersing the sample compartment into melting octan-2-ol, octan-1-ol and ice, respectively. Cooling of the sample compartment had two advantages. Firstly, by lowering the saturated gas pressure over the compound it was possible to achieve a better metering function of the valve. On the other hand, varying the temperature of the sample compartment allowed us to control the ratio of the two acetaldoxime isomers in the vapour (and consequently, in the matrix), as will be stressed later. This facilitated the interpretation and assignment of the experimental spectra.

Theoretical methods

In the present study both DFT and *ab initio* MP2 methods were used to estimate relative conformational stabilities and harmonic vibrational frequencies. The DFT calculations were performed with the combined Becke's three-parameter exchange functional[19] and the gradient-corrected correlation functional of Lee, Yang, Parr.[20] The standard 6-311++G** basis set as well as the Dunning's correlation-consistent double-zeta basis set augmented with s and p diffuse functions on hydrogen and s, p and d diffuse functions on heavy atoms (the aug-cc-pVDZ basis set) and the triple-zeta basis set augmented with s, p and d diffuse functions on hydrogen and s, p, d and f diffuse functions on heavy atoms (the aug-cc-pVTZ basis set)[21–23] were used in the calculations. All the DFT and MP2 calculations were performed using the Gaussian 98 program package.[24]

At each of the applied theory levels, the geometries of all possible (eight) C_s structures of acetaldoxime were fully optimized with the "tight" convergence threshold criteria. The geometry optimizations were followed by harmonic frequency calculations at the corresponding levels of theory. The calculated frequencies were used to assist in the analysis of the experimental spectra and to account for the zero-point vibrational energy (ZPVE) contribution.

A set of internal coordinates was defined and the Cartesian force constants were transformed to the internal coordinates space, allowing ordinary normal-coordinate analysis to be performed as described by Schachtschneider.[25] Internal coordinates used in these calculations are given in Table S1 (ESI).†

Results and discussion

Theoretical study of the potential energy surface

The central C=N double bond in the acetaldoxime molecule forces the O, N, C, C and H9 atoms to be coplanar. Hence, all isomers of this compound have C_s symmetry. The possible structures of acetaldoxime and their 3-letter designations are shown in Schemes 1 and 2 (*E* and *Z* families). By changing the configuration around the C–C, C=N or N–O bonds one of the isomers transforms into the other. Hence, the structures of acetaldoxime isomeric forms can be unambiguously described by the values of the dihedral angles HCCN, CC=NO and C=NOH. In the present paper we use small letters c (*cis*) and t (*trans*) for isomers appearing due to rotation around single bonds CC and NO, and capital letters *Z* (*zusammen*) and *E* (*entgegen*) to name the isomers differing by the configuration of the substituents around the double C=N bond.

The potential energy surface (PES) of acetaldoxime was studied theoretically at the MP2 and DFT(B3LYP) levels. Four minima and four first order saddle points were located. Two of the minima, the cEc and tZc forms, with *cis* orientation of

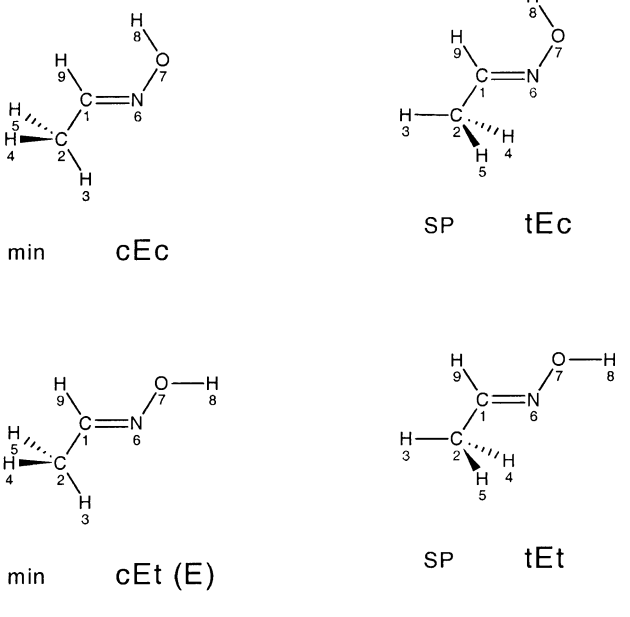

Scheme 1 Relevant structures of acetaldoxime with the *E* orientation around the C=N bond. SP, saddle point (for rotation of the methyl group); min, minimum.

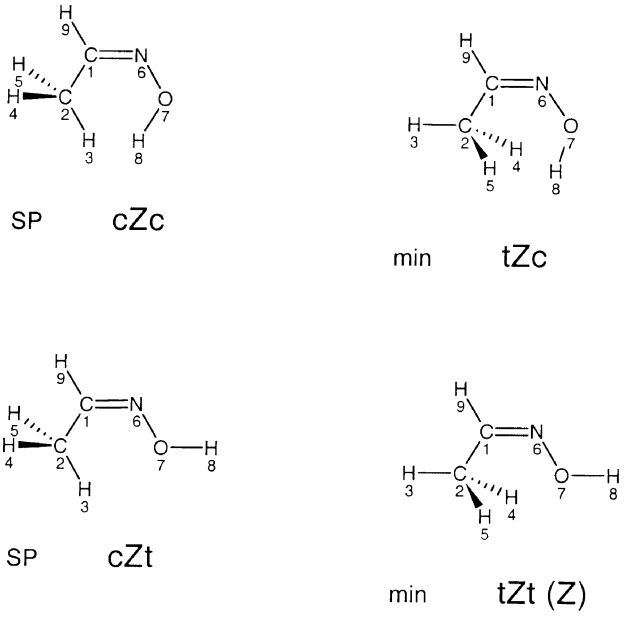

Scheme 2 Relevant structures of acetaldoxime with the *Z* orientation around the C=N bond. SP, saddle point (for rotation of the methyl group); min, minimum.

the OH group with respect to the C=N bond, have very high relative energies (see Table 1) and are of no practical interest. The calculated energies of the remaining two minima, cEt and tZt, are quite similar. When ZPVE is taken into account, both

Table 1 Energies (au) of the lowest energy isomer *E* and relative stabilities including the zero point vibrational energy (kJ mol^{-1}) of the acetaldoxime isomers calculated at the different levels of theory[a]

Method	cEt (*E*)	tZt (*Z*)	cEc	tZc
MP2/6-311++G**	−208.550317	0.92	21.97	28.46
MP2/aug-cc-pVDZ	−208.512273	0.14		
DFT(B3LYP)/6-311++G**	−209.132895	2.05	22.49	29.94
DFT(B3LYP)/aug-cc-pVDZ	−209.098332	2.23		
DFT(B3LYP)/aug-cc-pVTZ	−209.152850	2.56		

[a] All relative energies were calculated with respect to the isomer *E*.

MP2 and DFT calculations predict the cEt isomer as the global minimum (Table 1). The energy of the tZt isomer is only slightly higher than that of the cEt form and at all the applied levels of theory, the energy difference between these two forms is less than 2.6 kJ mol^{-1}. It is then clear that only these two isomers are important for further consideration. That is why, in the text below, we shall use the simplified notation: *E* for the cEt form and *Z* for the tZt form. The optimized geometrical parameters, calculated dipole moments and rotational constants of the two lowest energy forms of acetaldoxime are presented in Table 2. We shall stress here the good agreement between the theoretically calculated rotational constants and those measured experimentally by microwave spectroscopy.[10] This result supports the correctness of the assignment of the observed microwave spectra to the *E* and *Z* isomers of acetaldoxime.

The *Z*–*E* isomerization in acetaldoxime has been the subject of considerable theoretical interest. As early as 1930, Hückel[26]

Table 2 Optimized geometry parameters (Å and degrees), rotational constants (MHz), and dipole moments (D) calculated at the DFT(B3LYP)/6-311++G** and MP2/6-311++G** levels for acetaldoxime *E* and *Z* Isomers

	E			*Z*		
	DFT	MP2	Exp.[a]	DFT	MP2	Exp.[a]
Bond lengths						
C1C2	1.4945	1.4950		1.4988	1.4990	
C1N6	1.2706	1.2829		1.2742	1.2870	
C1H9	1.0925	1.0928		1.0866	1.0867	
C2H3	1.0904	1.0914		1.0901	1.0906	
C2H4	1.0949	1.0944		1.0939	1.0942	
C2H5	1.0949	1.0944		1.0939	1.0942	
N6O7	1.4102	1.4054		1.4106	1.4038	
O7H8	0.9630	0.9621		0.9629	0.9622	
Bond angles						
C2C1N6	120.2071	119.3760		126.5295	125.4935	
C2C1H9	119.6625	120.6486		120.2829	121.3957	
C1C2H3	110.6347	110.0554		110.9245	110.6889	
C1C2H4	110.5134	110.3839		110.5206	110.2434	
C1C2H5	110.5134	110.3839		110.5206	110.2434	
C1N6O7	111.3399	110.6940		111.3188	110.4737	
N6O7H8	102.9353	102.0721		102.7224	101.9080	
Dihedral angles						
N6C1C2H3	0.0	0.0		180.0	180.0	
N6C1C2H4	120.815	120.5585		−58.8878	−58.9187	
N6C1C2H5	−120.815	−120.5585		58.8878	58.9187	
H9C1C2H3	180.0	180.0		0.0	0.0	
C2C1N6O7	180.0	180.0		0.0	0.0	
C1N6O7H8	180.0	180.0		180.0	180.0	
Rotational constants						
A	46 370.9	45 581.4	44 613	17 370.9	17 197.1	17 364
B	4222.5	4239.9	4237.73	6558.8	6660.9	6658.92
C	3965.0	3975.0	3973.81	4904.4	4947.8	4921.04
Dipole moments						
μ	0.91	1.22	0.938	0.83	1.06	0.850

[a] Experimental rotational constants and dipole moment from ref. 10.

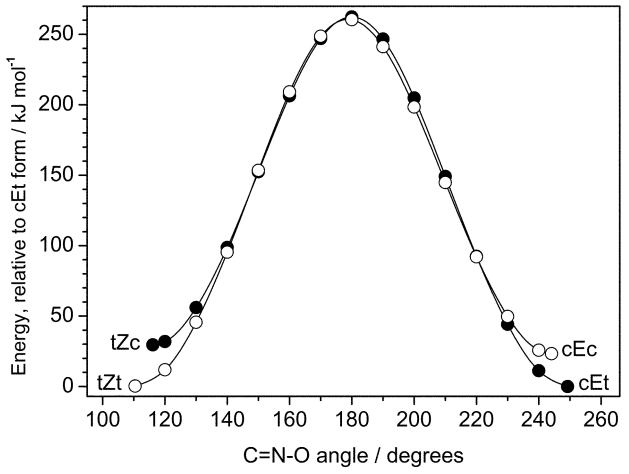

Fig. 1 Potential energy profile for the lateral shift of OH group in acetaldoxime calculated at the MP2/6-311++G** level of theory. Directions of the reaction pathway: white circles, from tZt to cEc form; black circles, from cEt to tZc form. In both cases reorientation of the methyl group relatively to the double bond happens when the reaction coordinate (C=N–O angle) is 120°.

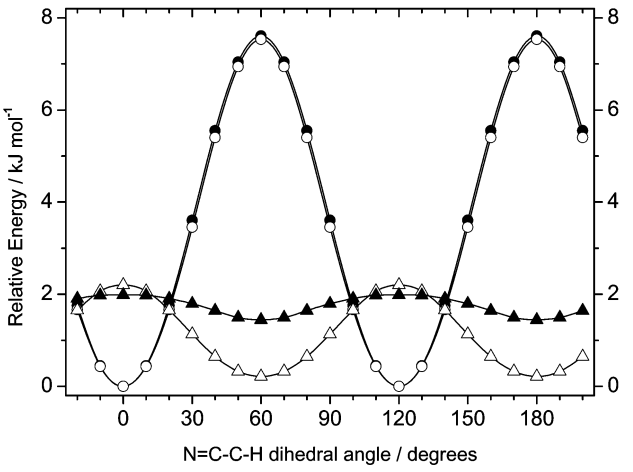

Fig. 2 Calculated barriers for the rotation of methyl group in acetaldoxime. White circles, *E*-isomer, MP2/6-311++G** calculation; black circles, *E*-isomer, DFT(B3LYP)/6-311++G** calculation; white triangles, *Z*-isomer, MP2/6-311++G** calculation; black triangles, *Z*-isomer, DFT(B3LYP)/6-311++G** calculation. Zero level for MP2 calculations corresponds to −208.623430 au and for DFT calculations to −209.205249 au. Zero-point vibrational energy is not included. An extended version of this figure (Fig. S2) is available as ESI.†

suggested that interconversion may take place by torsional motion (180° rotation around the C=N bond) or by inversion (lateral shift of the substituent linked to the imino group). A number of theoretical studies[27–30] agreed that the inversion mechanism in imine systems has a lower activation energy than the rotation around the double bond. For example, the energy barriers for inversion and rotation in acetaldoxime were calculated at the STO-3G level of theory to be 256.5 and 413.4 kJ mol^{-1}, respectively.[29]

In the present work we undertook an attempt to calculate the torsion and inversion barriers for *E*–*Z* isomerization at the higher level of theory (MP2/6-311++G**). The calculated shapes of the inversion barrier are presented in Fig. 1. During the calculation of the inversion reaction pathway, no restriction of symmetry was applied, but the molecule kept negligible deviations from C_s symmetry at all calculated points. Our results show that the heights (262 and 260 kJ mol^{-1}) of the barriers are practically direction independent.

We have also tried to calculate the reaction path for rotation around the C=N bond, but for geometries corresponding to C–C=N–O dihedral angles near 75° and 115° (depending on the direction of reaction) the heavy atoms backbone collapses to a planar structure. An analogous collapse happens if the H–C=N–O dihedral angle is used as the reaction coordinate. This is clear evidence that the torsional mechanism does not occur in the isolated molecule. Hence, our results support the idea that the inversion mechanism corresponds to the reaction path for isomerization in the studied molecule.

For an isolated molecule of acetaldoxime, a barrier for the inversion as high as 260 kJ mol^{-1} must preclude any interconversion between the *E* and *Z* forms at moderate temperatures. Indeed, as will be shown below, we did not see any evidence of *Z*–*E* isomerization in the gaseous phase. The mechanism of the previously observed transformations of the *E* form into the *Z* (or *vice versa*) in the condensed phases must then involve effects of intermolecular interactions, most probably proton exchange leading to transition state structures with a single C–N bond or carbanions.[4]

Another relevant structural feature in both *E* and *Z*-acetaldoxime is the orientation of the methyl group. For both isomers, the potential energy profiles with respect to the methyl rotation were calculated at the DFT(B3LYP) and MP2 levels, using the 6–311++G** basis set. Resulting energy curves are shown in Fig. 2 (extended version of this figure, presenting also the results obtained in DFT and MP2 calculations with aug-cc-pVDZ and aug-cc-pVTZ basis sets, is available as Fig. S2 in the ESI†). In these calculations, the value of the HCCN torsional angle was kept constant at each point while all remaining geometrical parameters were optimized. For the *E* isomer the calculated barrier height was 7.61 kJ mol^{-1} (DFT) and 7.53 kJ mol^{-1} (MP2). That corresponds very well to the experimental value 7.68 kJ mol^{-1} obtained by microwave spectroscopy.[10] The calculated barrier for the methyl rotation in the *Z* isomer is much lower: 0.54 kJ mol^{-1} (DFT) and 1.99 kJ mol^{-1} (MP2). The experimental value, 1.57 kJ mol^{-1}, estimated by Rogowski and Schwendeman,[10] lies in between the predictions of the two employed theoretical methods.

Infrared spectra of matrix isolated acetaldoxime

In the experimental investigations carried out in the present work, several low-temperature argon matrixes containing iso-

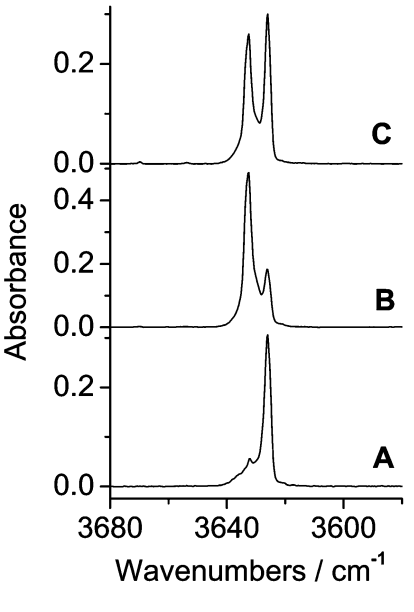

Fig. 3 High frequency fragment of the infrared spectra of acetaldoxime isolated in Ar matrix: A, deposition in the series III experiments; B, deposition in series II; C, deposition in series I; see description of the experimental details in the text.

lated acetaldoxime molecules were prepared and monitored by FTIR spectroscopy. The apparent feature noticed in the course of these experiments was the strong dependence of the ratio of the *E* and *Z* forms frozen in a matrix on the method of sample preparation. Three basic types of sample preparation were employed.

In the series I experiments, the vapour of acetaldoxime was premixed with argon (1 : 1000) in a vacuum line. The saturated vapour over the liquid sample of acetaldoxime (previously degassed) was used in this procedure. It has been checked that the *E* to *Z* ratio in the resulting matrix did not change from one mixture to the other, prepared several days later from a sample remaining liquid (at room temperature) only under the pressure of its saturated vapour. The high frequency fragment of the IR spectrum of acetaldoxime isolated in an Ar matrix, prepared as described above, is presented in Fig. 3 (trace C). Only one band due to the stretching vibration of the OH group should be expected in this range in the spectrum of a single isomer. Observation of two bands, separated by 6.6 cm^{-1}, suggests the coexistence of the *E* and *Z* forms frozen in the matrix.

In the series II experiments, argon and acetaldoxime vapours were introduced separately into the cryostat chamber. In this case, liquid acetaldoxime in a glass tube was frozen and kept at one of the temperatures: −39, −19 or 0 °C. Then the vapour over the solid passed through a needle valve and was deposited onto a cold matrix substrate together with the excess of argon coming from a separate line. In the resulting matrix, the ratio of the two νOH bands (Fig. 3, trace B) was significantly different from that obtained in series I. This result indicates a different *E*/*Z* ratio in the vapour over the frozen compound.

The method of matrix preparation in series III was similar to that just described. Gaseous acetaldoxime was also obtained as a vapour over a solid kept in the same type of glass tube, connected to the cryostat chamber through the same needle valve. The important difference was that the solid was not obtained by freezing the liquid a short time before matrix deposition, but was loaded into the glass tube as a solid (without giving it an opportunity to melt) from a solid sample, previously kept for many days in a refrigerator. The νOH range of the IR spectrum of a matrix prepared by this manner is strikingly different from those obtained in the two previous series of experiments (Fig. 3, trace A). The observed ratio of the two bands leaves no doubt that the ratio of *E* to *Z* forms was shifted very much in favour of one of the forms, and that this ratio is quite opposite to that observed in series II of the experiments.

In order to assign the two sets of bands observed in all three series of experiments to the two isomers of acetaldoxime, the experimental spectra were compared with the results of theoretical simulations carried out for both forms at DFT and MP2 levels. The frequencies and intensities of the IR bands calculated using these methods are collected in Tables 3 and 4. The frequencies and relative intensities of the bands observed in the experimental spectra are also provided in these tables. The 1500–1200 cm^{-1} regions of the experimental spectra

Table 3 Experimental and theoretically (DFT(B3LYP)/6-311++G** and MP2/6-311++G**) calculated frequencies[a] and intensities of the bands in the IR spectrum of the *E* form of acetaldoxime

Ar matrix		DFT calculations			MP2 calculations		
$\tilde{\nu}_{obs}$ cm^{-1}	*I* rel.	$\tilde{\nu}_{calc}$ cm^{-1}	A^{th} km mol^{-1}	PED %	$\tilde{\nu}_{calc}$ cm^{-1}	A^{th} km mol^{-1}	PED %
3632.8	116	3744.2	98	νOH(100)	3758.4	101	νOH(100)
3069.4	1						
3033.2	4	3049.8	13	νCH_3asym(93)	3088.5	9	νCH_3asym(97)
3006.7	10	3010.9	12	νC1H(97)	3046.2	10	νC1H(98)
2989.3	3						
2959.9	17	2996.1	15	νCH_3asym′(100)	3052.0	11	νCH_3asym′(100)
2931.1	14	2950.3	19	νCH_3sym(95)	2977.7	16	νCH_3sym(98)
1663.9	2	1686.2	1	νC=N(79)	1641.4	0.1	νC=N(74)
1446.8	14	1446.1	13	δCH_3asym(87)	1456.4	10	δCH_3asym(74)
1443.2	12	1443.0	11	δCH_3asym′(92)	1446.6	10	δCH_3asym′(93)
1431.6	3						
1403.2	7	1400.7	5	δOH(29), δC1H(27), δCH_3sym(24)	1405.7	4	δOH(30), δCH_3sym(28), δC1H(25), νCC(11)
1376.5	4						
1366.0	34	1365.3	23	δCH_3sym(71), δOH(18), δC1H(10)	1362.6	22	δCH_3sym(67), δOH(20), δC1H(11)
1303.6	3						
1267.2	25						
1251.0	48	1254.6	54	δC1H(49), δOH(40), νC=N(12)	1249.9	53	δC1H(49), δOH(38), νC=N(14)
1133.5	8	1120.4	4	γCH_3(39), νCC(31), δNCC(18)	1127.6	3	γCH_3(36), νCC(34), δNCC(17)
1053.4	2	1054.6	1	γCH_3′(60), τC1H(35)	1046.8	2	γCH_3′(66), τC1H(29)
976.2	103	973.5	136	νNO(47), νCC(28), γCH_3(13)	987.4	116	νNO(54), νCC(22), γCH_3(12)
897.7	17	892.3	10	τC1H(67), γCH_3′(28)	880.5	12	τC1H(74), γCH_3′(23)
885.1 / 882.6	39	879.4	31	νNO(43), γCH_3(29), νCC(11)	886.0	16	νNO(37), γCH_3(34), νCC(12)
718.4	15						
714.6							
583.5	1						
554.7	18	551.5	16	δCNO(47), δNCC(21), νCC(17)	552.4	15	δCNO(49), δNCC(21), νCC(16)
		387.8	148	τOH(98)	332.1	129	τOH(83), τONCC(13)
		317.9	3	δNCC(59), δCNO(34)	316.8	2	δNCC(60), δCNO(33)
		281.3	1	τONCC(94)	267.0	19	τONCC(79), τOH(17)
		191.7	0.2	τCH_3(98)	183.9	0.01	τCH_3(97)

[a] Theoretical frequencies are scaled by 0.978 (DFT) and 0.968 (MP2).

Table 4 Experimental and theoretically (DFT(B3LYP)/6-311++G** and MP2/6-311++G**) calculated frequencies[a] and intensities of the bands in the IR spectrum of the *Z* form of acetaldoxime

Ar matrix		DFT calculations			MP2 calculations		
$\tilde{\nu}_{obs}$ cm^{-1}	*I* rel.	$\tilde{\nu}_{calc}$ cm^{-1}	A^{th} km mol^{-1}	PED %	$\tilde{\nu}_{calc}$ cm^{-1}	A^{th} km mol^{-1}	PED %
3626.2	87	3746.0	99	νOH(100)	3756.5	103	νOH(100)
3049.7	7	3081.1	9	νC1H(95)	3118.0	7	νC1H(94)
3002.9	6	3047.6	13	νCH$_3$asym(93)	3090.7	10	νCH$_3$asym(93)
2971.7	9	3010.1	9	νCH$_3$asym′(100)	3055.8	6	νCH$_3$asym′(100)
2934.7	9	2961.0	9	νCH$_3$sym(97)	2953.6	9	νCH$_3$sym(98)
1661.8	4	1681.3	8	νC=N(77)	1636.4	3	νC=N(71)
1450.5	9	1446.4	9	δCH$_3$asym(85)	1454.5	8	δCH$_3$asym(86)
1444.2	22	1440.6	11	δCH$_3$asym′(92)	1442.3	10	δCH$_3$asym′(93)
1374.3	19	1374.5	13	δCH$_3$sym(85)	1377.2	13	δCH$_3$sym(85)
1335.6	35	1328.9	37	δOH(67), δC1H(20)	1329.9	37	δOH(66), δC1H(19)
1295.8	35	1303.7	47	δC1H(63), δOH(20), νC=N(13)	1296.5	43	δC1H(63), δOH(18), νC=N(16)
1104.0	26	1085.4	18	γCH$_3$(45), νCC(20), δNCC(19)	1096.0	12	γCH$_3$(41), νCC(25), δNCC(19)
		1030.9	0.4	γCH$_3$′(68), τC1H(25)	1019.4	1	γCH$_3$′(73), τC1H(20)
942.7 919.0	20 27	940.8	37	νCC(49), γCH$_3$(25), νNO(14)	953.3	41	νCC(39), γCH$_3$(28), νNO(20)
887.6	65	885.5	86	νNO(79), νCC(13)	906.9	57	νNO(73), νCC(17)
855.8 839.9 834.1 825.2	54	827.0	20	τC1H(81), γCH$_3$′(16)	812.2	20	τC1H(85), γCH$_3$′(12)
745.3	9						
730.3	6						
669.2 666.1 663.5	15	669.5	16	δCNO(49), δNCC(21), γCH$_3$(13)	666.3	15	δCNO(51), δNCC(22), γCH$_3$(13)
493.8 487.0 483.3	33	510.4	42	τONCC(58), τOH(40)	484.1	26	τONCC(69), τOH(28)
		395.5	89	τOH(60), τONCC(41)	340.1	107	τOH(72), τONCC(28)
		276.8	1	δNCC(59), δCNO(38)	283.0	2	δNCC(59), δCNO(37)
		52.1	0.05	τCH$_3$(100)	77.5	0.03	τCH$_3$(99)

[a] Theoretical frequencies are scaled by 0.978 (DFT) and 0.968 (MP2).

obtained in the series I, II and III experiments are shown in Fig. 4, together with the corresponding region of the DFT-simulated spectra for the *Z* and *E* isomers. The agreement between the experimental and theoretical spectra allows an unequivocal assignment of the form dominating in the series II experiments to the *E* isomer and of the form dominating in the series III to the *Z* form. Simple operations (subtractions with a scale factor) on the experimental spectra resulting from the series II and III experiments allowed us to obtain the experimental spectra of pure *E* and pure *Z* isomers. These are presented in Figs. 5 and 6, where they are compared with the corresponding theoretical spectra. In the case of the *E* isomer the experimental spectrum is very well reproduced by the theoretical simulation. The strongest band at 976.2 cm^{-1} is interpreted as due to the stretching vibration of the NO bond. Strong bands at this frequency, corresponding to the νNO vibration, are very typical for the spectra of oximes.[31,32] The pair of bands at 718.4 and 714.6 cm^{-1}, which has no counterpart in the spectrum calculated within the harmonic approximation, can be ascribed to the overtone of the τOH fundamental tone, with a predicted frequency of 387.8 cm^{-1}. An analogous interpretation could be made in order to explain the bands at 745.3 and 730.3 cm^{-1} in the spectrum of the *Z* form.

The overall agreement between the experimental spectrum of the *Z* isomer and the corresponding spectrum predicted within the harmonic approximation is somewhat worse than in the case of the *E* form. Observation of multiple splittings in several bands due to the *Z* isomer suggests the presence of some significant anharmonic effect in this form. In all probability, the nearly free rotation of the methyl group in this isomer (see Fig. 2) accounts for the observed splittings. Indeed, the very low barrier for the internal rotation of the methyl group (1.57 kJ mol^{-1})[10] will allow large amplitude torsional vibrations of the three methyl hydrogen atoms. That is in agreement with the very low (52 cm^{-1}) theoretically predicted frequency for the CH$_3$ torsion in the *Z* form. On the contrary, for the *E* isomer, where the barrier for the methyl group rotation is nearly 5 times higher than in the *Z* form, no significant distortions from the harmonic theoretical simulation can be noticed in the experimental IR spectrum.

All our experiments indicate that for the molecules in the gas phase there is no interconversion between the two isomers. Gaseous acetaldoxime coming to the cold matrix substrate was, in all the experiments, at the same room temperature, but the *E* to *Z* ratio frozen in a matrix was dramatically different in the different series of experiments. The fact that very different relative populations of the *E* and *Z* forms of acetaldoxime were frozen in the matrixes in the three series of experiments described above, can be interpreted as a result of the combination of two factors: the composition of the solid or liquid acetaldoxime sample and the relative evaporation speeds of the *E* and *Z* isomers.

It was already known from previous investigations,[9] that the *E* to *Z* ratio in the acetaldoxime neat liquid is similar to that observed in the present work in the matrixes prepared (series I) from the vapour over the liquid compound. Analogously, solid acetaldoxime kept for several days in a refrigerator

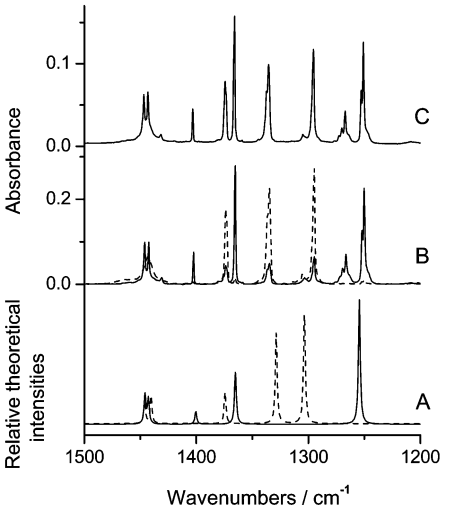

Fig. 4 The "fingerprint" fragment of the infrared spectra of acetaldoxime: A, solid line, spectrum of the *E*-form calculated at the DFT(B3LYP)/6-311++G** level, dashed line, spectrum of the *Z*-form calculated at the same level; B, experimental spectra: solid line, deposition in the series II experiments, dashed line, deposition in series III; C, experimental spectra, deposition in series I; see description of the experimental details in the text; theoretically calculated frequencies were scaled by 0.978.

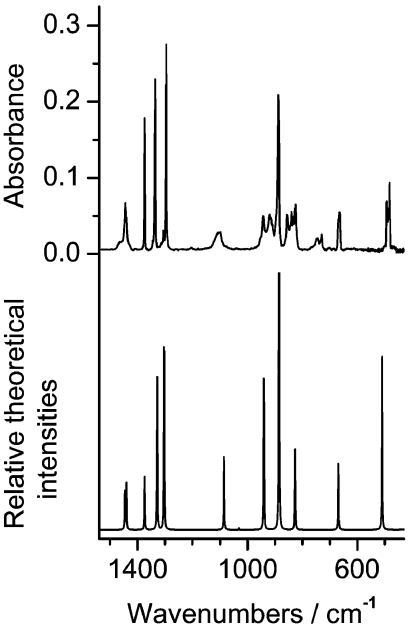

Fig. 6 Comparison of the experimental spectrum of the *Z*-form of acetaldoxime isolated in an Ar matrix (upper panel), with the spectrum of this isomer theoretically calculated at the DFT(B3LYP)/6-311++G** level (lower panel); theoretically calculated frequencies were scaled by 0.978.

should adopt the *Z* form,[13] and just this form has been found as highly dominating in the matrixes prepared by evaporation of the solid compound previously kept for some days at temperatures below 0 °C (series III). The observation of the domination of the *E* isomer in matrixes prepared from the vapour over the freshly frozen solid (series II) does not necessarily reflect the composition of the source solid. Indeed, after freezing, the compound tends to adopt the *Z* form,[13] which contradicts the observation of more populated *E* form. Moreover, in the series II of experiments, we observed a dependence of the *E* to *Z* ratio in the matrixes on the temperature of the source solid: the lower this temperature, the higher the relative amount of the *E* form. Let us assume that during freezing of the acetaldoxime the *E* and *Z* isomers form their crystals independently, *i.e.* behave as two different compounds. In this case, if the saturated vapour pressure over the *Z* form of solid acetaldoxime diminishes with decreasing temperature faster than for the *E* form, it is easy to explain both the temperature dependence observed in series II of our experiments and the prevalence of the *E* form in that series.

To provide better insight into the behaviour of acetaldoxime we have undertaken further studies. Recently, we investigated various crystalline phases of the compound by means of infrared spectroscopy, differential scanning calorimetry and thermomicroscopy. A paper describing these studies is currently in preparation.

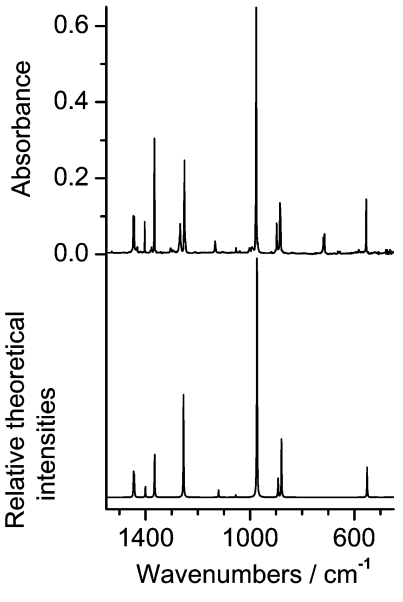

Fig. 5 Comparison of the experimental spectrum of the *E*-form of acetaldoxime isolated in an Ar matrix (upper panel), with the spectrum of this isomer theoretically calculated at the DFT(B3LYP)/6-311++G** level (lower panel); theoretically calculated frequencies were scaled by 0.978.

Conclusion

This work reports the experimental infrared spectra of acetaldoxime isolated in inert matrixes of solid argon. The spectral signatures of the *Z* and *E* monomers of the compound have been unequivocally identified for the first time. The interpretation of the experimental spectra was assisted by *ab initio* MP2/6-311++G** and DFT(B3LYP)/6-311++G** calculations. The *Z* form was shown to exhibit a very low barrier for rotation of the methyl group. It was also found that there is no interconversion between the *E* and *Z* isomers of acetaldoxime in the gaseous phase at room temperature and below. Furthermore, it was shown that the composition of the samples is strongly dependent on the method of their preparation.

Acknowledgement

The financial support of the *Fundação para a Ciência e a Tecnologia*, Lisbon (grant FCT #SFRH/BPD/1661/2000 and research project POCTI/43366/QUI/2001) is acknowledged. I. Reva is grateful to Dr. Douglas J. Fox for valuable suggestions concerning optimization of the performance of the Gaussian program.

References

1 T. J. Venanzi and C. A. Venanzi, *J. Comput. Chem.*, 1988, **9**, 67–74.
2 E. M. Acton and H. Stone, *Science*, 1976, **193**, 584–586.
3 J. W. Smith, in *The Chemistry of the Carbon–Nitrogen Double Bond*, ed. S. Patai, Wiley-Interscience, New York, 1970, p. 235.
4 R. Glaser and A. Streitwieser, *J. Am. Chem. Soc.*, 1989, **111**, 7340–7348.
5 K. B. Wiberg and R. Glaser, *J. Am. Chem. Soc.*, 1992, **114**, 841–850.
6 M. T. Nguyen and T.-K. Ha, *J. Mol. Struct.*, 1982, **88**, 127–136.
7 P. Kolandaivel and K. Senthilkumar, *J. Mol. Struct. (THEOCHEM)*, 2001, **535**, 61–70.
8 R. Harris and R. C. Rao, *Org. Magn. Res.*, 1983, **21**, 580–586.
9 G. Geiseler, H. Böhlig and J. Fruwert, *J. Mol. Struct.*, 1973, **18**, 43–48.
10 R. S. Rogowski and R. H. Schwendeman, *J. Chem. Phys.*, 1969, **50**, 397–403.
11 O. Ohashi, R. Ishihara, K. Murakami, T. Sakaizumi, M. Onda and I. Yamaguchi, *Bull. Chem. Soc. Jpn.*, 1976, **49**, 891–893.
12 M. M. Caldeira and V. M. Gil, *Tetrahedron*, 1976, **32**, 2613–2615.
13 W. R. Dunstan and T. S. Dymond, *J. Chem. Soc.*, 1892, **61**, 470–473.
14 R. E. Gawley and T. Nagy, *Tetrahedron Lett.*, 1984, **25**, 263–264 and 3506.
15 C. E. Holloway and C. P. J. Vuik, *Tetrahedron Lett.*, 1979, **12**, 1017–1020.
16 T. Okuda, Y. Yano, A. Ueda, H. Terao and K. Yamada, *J. Mol. Struct.*, 1992, **273**, 269–276.
17 D. Hadži and L. Premru, *Spectrochim. Acta, Part A*, 1967, **23**, 35–44.
18 I. D. Reva, S. G. Stepanian, L. Adamowicz and R. Fausto, *J. Phys. Chem. A*, 2001, **105**, 4773–4780.
19 A. D. Becke, *Phys. Rev. B*, 1988, **38**, 3098–3100.
20 C. Lee, W. Yang and R. G. Parr, *Phys. Rev. B*, 1988, **37**, 785–789.
21 D. E. Woon and T. H. Dunning, *J. Chem. Phys.*, 1993, **98**, 1358–1371.
22 R. A. Kendall, T. H. Dunning and R. J. Harrison, *J. Chem. Phys.*, 1992, **96**, 6796–6806.
23 T. H. Dunning, *J. Chem. Phys.*, 1989, **90**, 1007–1023.
24 M. J. Frisch, G. W. Trucks, H. B. Schlegel, G. E. Scuseria, M. A. Robb, J. R. Cheeseman, V. G. Zakrzewski, J. A. Montgomery, Jr., R. E. Stratmann, J. C. Burant, S. Dapprich, J. M. Millam, A. D. Daniels, K. N. Kudin, M. C. Strain, O. Farkas, J. Tomasi, V. Barone, M. Cossi, R. Cammi, B. Mennucci, C. Pomelli, C. Adamo, S. Clifford, J. Ochterski, G. A. Petersson, P. Y. Ayala, Q. Cui, K. Morokuma, D. K. Malick, A. D. Rabuck, K. Raghavachari, J. B. Foresman, J. Cioslowski, J. V. Ortiz, A. G. Baboul, B. B. Stefanov, G. Liu, A. Liashenko, P. Piskorz, I. Komaromi, R. Gomperts, R. L. Martin, D. J. Fox, T. Keith, M. A. Al-Laham, C. Y. Peng, A. Nanayakkara, M. Challacombe, P. M. W. Gill, B. Johnson, W. Chen, M. W. Wong, J. L. Andres, C. Gonzalez, M. Head-Gordon, E. S. Replogle and J. A. Pople, *Gaussian 98, Revision A.9*, Gaussian Inc., Pittsburgh PA, 1998.
25 J. H. Schachtschneider, Technical Report, Shell Development Co. Emeryville, CA, 1969.
26 E. Hückel, *Z. Phys.*, 1930, **60**, 423–456.
27 F. Kerek, G. Ostrogovich and Z. Simon, *J. Chem. Soc. B*, 1971, 541–544.
28 D. Liotard, A. Dargelos and M. Chaillet, *Theoret. Chim. Acta*, 1973, **31**, 325–333.
29 G. Leroy, M.-T. Nguyen, M. Sana and J.-L. Villaveces, *Bull. Soc. Chim. Belg.*, 1980, **89**, 1023–1037.
30 R. D. Bach and G. J. Wolber, *J. Org. Chem.*, 1982, **47**, 245–248.
31 T. Stepanenko, L. Lapinski, M. J. Nowak and L. Adamowicz, *Vib. Spectrosc.*, 2001, **26**, 65–82.
32 L. Lapinski, M. J. Nowak and L. Adamowicz, *Photochem. Photobiol.*, 2001, **74**, 253–260.